Article

Response Characteristics of Weak Current Stimulated from Coal under an Impact Load and Its Generation Mechanism

Dexing Li [1,2,3,*], Enyuan Wang [1,2], Dianqi Jin [3], Dongming Wang [1,2] and Wei Liang [3]

1   Key Laboratory of Gas and Fire Control for Coal Mines (China University of Mining and Technology), Ministry of Education, Xuzhou 221116, China
2   School of Safety Engineering, China University of Mining and Technology, Xuzhou 221116, China
3   Shenzhen Urban Public Safety Technology Research Institute Co., Ltd., Shenzhen 518000, China
*   Correspondence: ldx3180@cumt.edu.cn

Abstract: Understanding the response law and mechanism of weak currents stimulated from coal under an impact load is significant for the prediction of coal bumps in deep coal mines. In this paper, the system for the weak current measurement of coal under an impact load is established and the response characteristics of weak currents induced by the deformation of coal under an impact load are investigated. Physical models are established to describe the process of charge transfer and explain the generation mechanism of those currents. The results show that a transient current is stimulated from the coal sample when an impact load is applied, and then, the current decays slowly, tending to be a stable value that is slightly greater than the background current. The weak current flows from the loaded volume to the unloaded volume of the coal and increases with the impact velocity in a negative exponential form. Analysis of weak currents using non-extensive entropy shows that the attenuation of the weak current obeys non-extensive statistical mechanics and the non-extensive parameter q is greater than 2. The carriers are mainly electrons, of which the distribution obeys the tip effect that electrons tend to enrich towards the tip of a crack. The generation mechanism of those weak currents induced by coal deformation is the instantaneous movement of electrons under a density difference caused by the tip effect. Research results can provide a new perspective to understand the electric phenomena of coal under an impact load as well as a new method for coal bump prediction.

Keywords: coal bump; transient current; impact load; mechanism; carriers

1. Introduction

Coal bumps, a kind of underground dynamic disaster induced by the sudden release of elastic deformation energy accumulated in coal mass during mining [1,2], usually cause serious casualties and property loss [3]. A coal bump is closely related to the deformation aggravation of coal mass [4–6], of which the process is always accompanied by the emission of various physical signals, such as acoustic emission (AE), electromagnetic radiation (EMR), surface potential, and charge induction, which can reflect the damage evolution of coal [4,7,8]. Therefore, the measurement of the physical signals emitted from coal during deformation is an important basis for coal bump prediction and early warning [9].

Applying a mechanical load on coal and rock materials can stimulate a weak current [10–16], which is also called the pressure stimulated current (PSC). Stavrakas et al. [11] studied the characteristics of PSC from marbles through laboratory experiments, which showed that an obvious weak current can be generated after the stress reaches $0.6\sigma_f$ (σ_f is the peak stress), and the peak current is considered to be proportional to the loading rate. Afterward, Triantis et al. [13] obtained a more general conclusion on the relationship between PSC and the mechanical behavior of loaded marble specimens: obvious weak currents can be observed only when the applied load exceeds the yield stress, and the

generation of weak current from rocks is mainly induced by the change in Young's modulus. Kyriazopoulos et al. [17] believe that the PSC is directly proportional to the strain rate, and the occurrence of fracture is accompanied by the sudden increase in PSC. The experimental results from a study by Freund et al. [14,15,18,19] on weak currents from igneous rocks (granite, anorthosite, gabbro, etc.) show that a weak current is generated the moment a load is applied, and it can increase rapidly to a peak even at a very low stress level. Li et al. [16] believe that PSC response characteristics are closely related to the deformation stages of rock; they also found that the precursors of rock failure based on the PSC response are different for various stress states, such as under progressive loading and during a creep process. In recent years, the weak current technique has been introduced to study the deformation and damage process of coals. He et al. [20,21] measured weak currents of nanoamps on the surface of coal samples under uniaxial compression, confirming that weak currents can also be stimulated from loaded coal. Li et al. [22] investigated the response laws of weak currents stimulated from large-scale coal samples under a concentrated load and proposed the principles of predicting coal bumps using the weak current method. To verify the feasibility of the weak current method in coal bump prediction, Li et al. [23] also conducted field tests in a deep underground coal mine using their self-developed weak current measuring device, filling the gap in the application of the weak current technique in underground engineering. The field test results show that the weak current responds well to mine seismicities and the weak current technique has a broad prospect in coal and rock dynamic disaster prediction due to its advantages of strong anti-interference ability and sensitive response.

Previous research on the weak current stimulated from stressed coals provides a new idea and theoretical basis for coal bump prediction and early warning, but almost all of these studies are focused on the static load condition. In underground mining, the catastrophic failure of coal under the disturbance induced by excavation blasting, mechanical drilling, and roof fracture is becoming one of the major safety risks [24,25]; thus, investigations on the measurement of the physical signals of coal under an impact load are vital for the further understanding of the coal bump evolution process. Liu et al. [26] investigated the burst characteristics of coal under impact loading using an AE system and analyzed the development of fractures in coal samples through an AE count. Feng et al. [27] studied the fracture characteristics of coal and its AE response under dynamic loading, revealing the "double peak" pattern of the dynamic strength of coals. Yang et al. [28] studied the damage evolution characteristics of coal samples under impact loading under different surrounding pressures by measuring the change in ultrasonic wave velocity, through which the internal damage of coal samples was quantitatively characterized. Xu et al. [29] investigated EMR characteristics during the dynamic fracturing progress of gas-bearing coal under impact loadings through laboratory experiments.

So far, the research on the weak current response characteristics of coal under an impact load is still lacking, which limits the improvement of the weak current technique for coal bump prediction and early warning. In the present work, an experimental system for the weak current measurement of coal under an impact load is established, laboratory experiments on coal samples under various impact loads are conducted, and the weak currents are measured synchronously. The response characteristics of the weak current are analyzed and its generation mechanism is investigated, by which the physical models are established to describe the processes of charge transfer and weak current generation.

2. Experimental Details

2.1. Material

Coal blocks were collected from the Zhangminggou coal mine in Shaanxi, China. Cuboid samples measuring $50 \times 80 \times 200$ mm^3 were cored and cut from these blocks in strict accordance with the standards specified by the International Society for Rock Mechanics [30]. The surfaces of each sample were ground flat so that the surface roughness

did not exceed ± 0.02 mm, and the end face was perpendicular to the axis; the maximum deviation was not greater than $0.25°$.

2.2. Experimental System

The experimental system consists of a loading system, a weak current measurement system, and an electromagnetic shielding system (Figure 1). The impact load is supplied by a DK-5621 falling ball impact tester, with the drop height ranging from 0 to 2000 mm, with a minimum scale of 10 mm. The drop of the ball is controlled by a DC solenoid valve with an infrared positioning function. The weak current measurement system consists of a Keithley 6517B electrometer (Tektronix (China) Co., Ltd., Shanghai, China), a computer, a tri-coaxial cable, and two electrodes. The range of this electrometer is from 1 fA to 20 mA, with a minimum resolution of 1 fA. The independently developed data acquisition software, based on the LabVIEW system design platform (National Instruments, Austin, TX, USA), is installed on a personal computer running Windows 10 to acquire, display, and store the current data. To diminish the interference of surrounding electrical noise to the weak currents generated from the coal samples, the experiments were conducted in an electromagnetic shielding room.
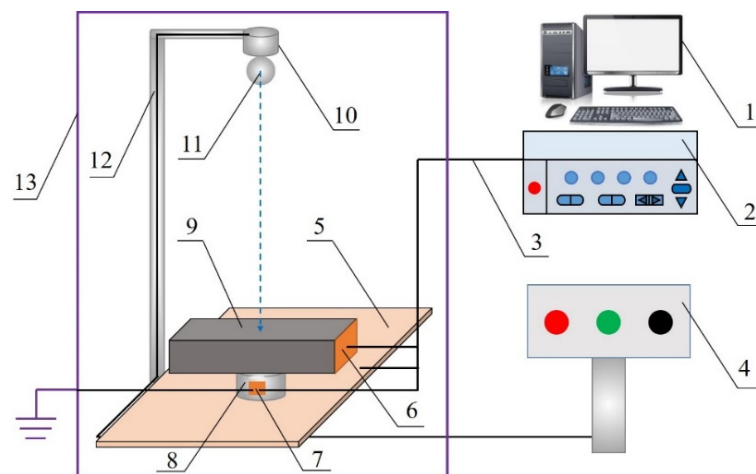

Figure 1. Diagrammatic sketch of impact loading and electrode arrangement. (1) Computer; (2) electrometer; (3) triaxial shielded cable; (4) solenoid valve controller; (5) Teflon sheet; (6,7) copper electrode; (8) stainless steel piston; (9) coal specimen; (10) DC solenoid valve; (11) steel ball; (12) fixed support; (13) electromagnetic shielded room.

2.3. Experimental Scheme

As shown in Figure 1, the sample measuring $50 \times 80 \times 200$ mm^3 is put on a steel piston of 80 mm in diameter that is electrically insulated from the tester by a 3-millimeter-thick Teflon sheet. An oblong copper electrode (80 mm long, 50 mm wide) is attached to the end surface of the unstressed volume, and another copper electrode (30 mm long, 20 mm wide) is attached to the steel piston. The HI (high) side of the electrometer is connected to the electrode attached to the end side of the unstressed volume, while the LO (low) side is connected to the electrode attached to the piston, which is also connected to an electromagnetically shielded room that is grounded. The sampling frequency of 3 Hz for the current measurement has been chosen in the experiments.

Five specimens numbered CIL01, CIL02, CIL03, CIL04, and CIL05 were prepared for impact loading tests. A steel ball weighing 225 g was used for the tests, and eight falling heights of 0.1, 0.2, 0.4, 0.5, 0.6, 0.8, 1.0, and 1.5 m were set to investigate the influence of impact velocity on the magnitude of transient currents. Three groups of parallel tests on Specimens CIL01, CIL02, and CIL03 were carried out; Specimens CIL04 and CIL05 were held in reserve.

3. Results and Discussion

3.1. Weak Current Response Characteristics

Figure 2 shows the variation of weak currents stimulated from Specimen CIL02 with time. It can be seen that before an impact load is applied to the coal sample, the weak current is stable at a certain value, which is called the background current. The moment an impact load is applied, the weak current increases instantly to the peak value; the phenomenon is known as a transient current. After that, the current decreases gradually, tending to be a certain value (marked by the dashed line), which is named the stable current. As shown in Figure 2, after an attenuation of hundreds of seconds, the current seems to be still greater than the stable current, which is verified by the data listed in Table 1. Previous research shows that the weak currents from rock and coal under a static load also decay when the applied load no longer increases or remains constant [12,13,16,19,22], and the decay trend is similar to that shown in Figure 2. The difference is that the stable current is much higher than the background one for the static load condition, while the two are very close for the impact load condition (see Table 1). Due to the fact that the applied load is the driving force of the generation of weak current, the current can also be stimulated, although the load applied on the coal/rock is maintained, making the current stable at a value much higher than the background one. In our experiments, the application of the impact load on the coal samples can be considered instantaneous and is removed subsequently, making the transient current decay without any driving force. Essentially, the weak current stimulated by an impact load tends to be the background value, but this process will take a long time, so the stable current is only a little higher than the background current.

Table 1. Typical currents stimulated from Specimen CIL02 under various impact loadings.

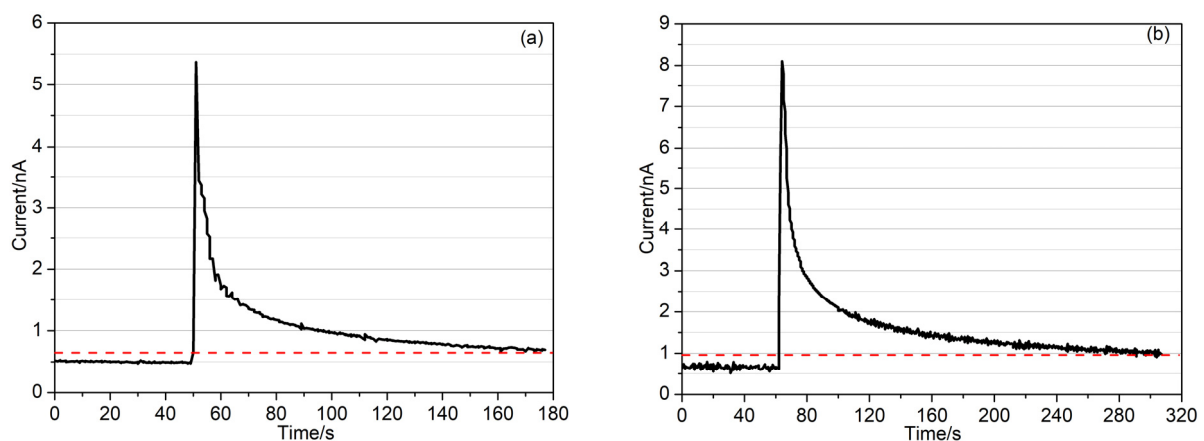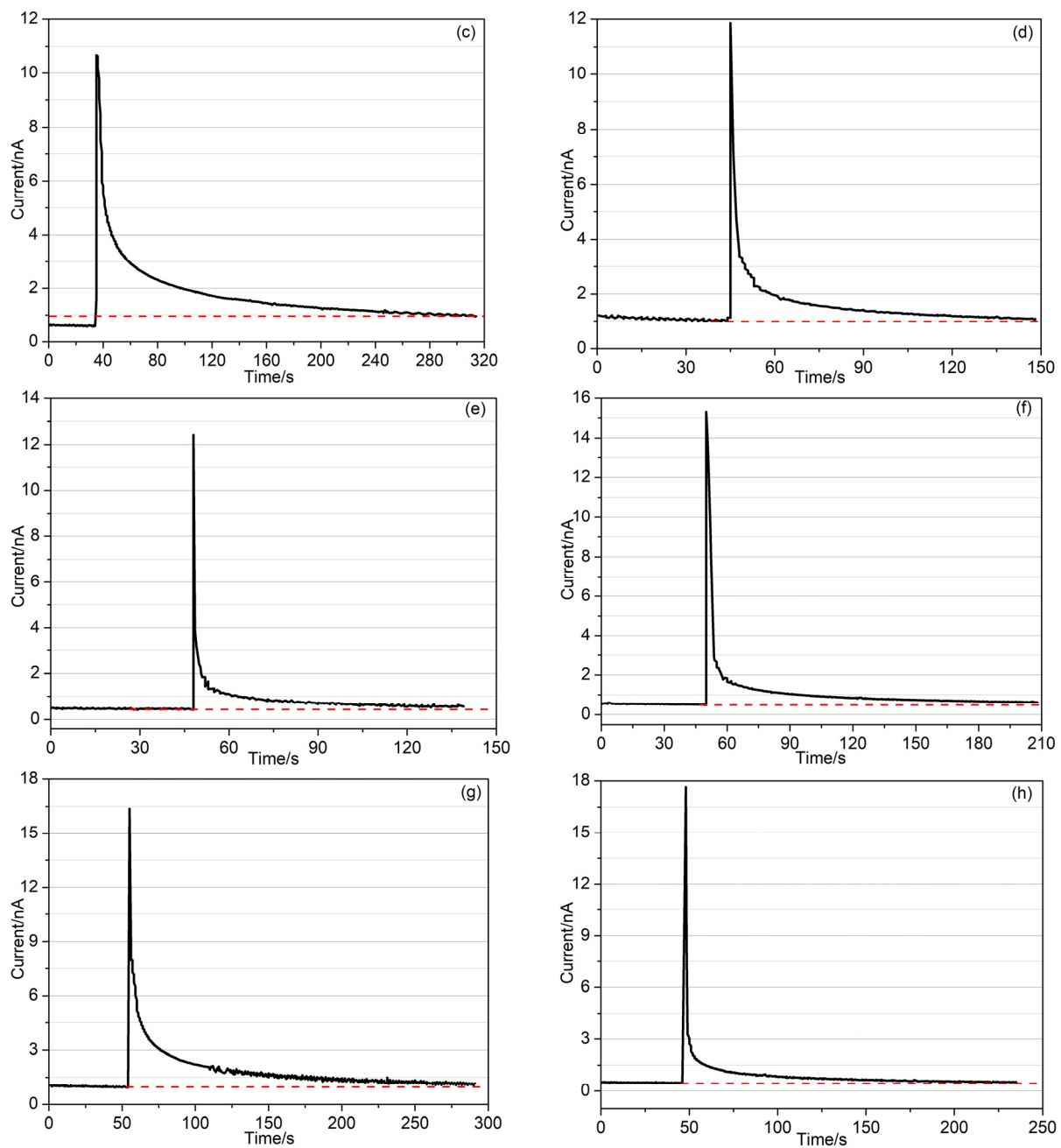| Drop Height/m	Background Current/nA	Peak Current/nA	Stable Current/nA
0.1	0.5	5.4	0.7
0.2	0.6	8.1	1.0
0.4	0.6	10.7	1.0
0.5	1.0	11.9	1.1
0.6	0.4	12.4	0.6
0.8	0.6	15.3	0.6
1.0	1.0	16.4	1.2
1.5	0.5	17.6	0.5

Figure 2. *Cont.*

Figure 2. Variation of weak currents with time for Specimen CIL02 for different ball falling heights. (**a**) 0.1 m; (**b**) 0.2 m; (**c**) 0.4 m; (**d**) 0.5 m; (**e**) 0.6 m; (**f**) 0.8 m; (**g**) 1.0 m; (**h**) 1.5 m. The dashed line marks the stable current.

It can be seen from Figure 2 that the variation law of weak currents stimulated from coals under an impact load is consistent, but the peak currents are different. Therefore, it is necessary to investigate the relationship between the falling height of the ball and the intensity of a transient current, which can be calculated by the following formula:

$$I_{tr} = I_{p} - I_{b} \tag{1}$$

where I_{tr} is the intensity of a transient current, I_{p} is the peak current, and I_{b} is the background current. The intensity of transient currents for the three groups of experiments is listed in Table 2, and the error bar curve is shown in Figure 3. The fitting results of the scatter of the average transient current show that the intensity of transient currents increases exponentially with the falling height of the ball.

Table 2. Intensity of transient current from coal samples under an impact load.

Drop Height/m	Transient Current/nA			
	CIL01	CIL02	CIL03	Average
0.1	3.8	4.9	4.3	4.3
0.2	9.4	7.5	7.4	8.1
0.4	13.1	10.1	10.6	11.5
0.5	14.4	10.9	12.1	12.5
0.6	13.5	12.0	14	13.2
0.8	15.6	14.7	14.8	15.0
1.0	14.7	15.4	17.2	15.8
1.5	19.5	17.1	16.3	17.6

$$I_{tr} = -16.5 \cdot e^{-2.5h} + 17.3, \quad R^2 = 0.995$$
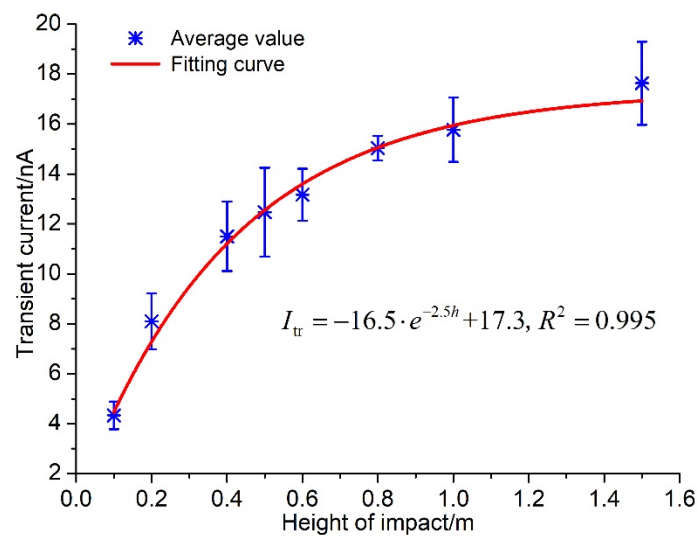
Figure 3. Error bar curve of transient currents with the falling height of the ball (*h*) for the three groups of tests.

Previous studies show that the weak current stimulated from coals under a static load increases with strain rate [22,30], so it is reasonable to investigate the relationship between the transient current and the strain rate of coal under an impact load.

According to the law of conservation of energy [31], the gravitational potential energy before the ball begins to fall is equal to the kinetic energy the moment it hits the coal sample without considering the effect of air resistance; hence, the energy relationship is

$$\frac{1}{2}mv^2 = mgh \tag{2}$$

where *m* is the mass of the ball, *g* is gravitational acceleration, *h* is the height the ball falls from, and *v* is the speed of the ball when hitting the coal sample. Then

$$v = \sqrt{gh} \tag{3}$$

The strain rate caused by the impact load is positively correlated with the speed of the ball when striking the coal sample [24], that is

$$\frac{d\varepsilon}{dt} \propto v \tag{4}$$

From Equations (3) and (4), we can derive Equation (5):

$$\frac{d\varepsilon}{dt} \propto h^{1/2} \tag{5}$$

In order to investigate the relationship between the transient current and the strain rate, the relationship between the transient current and $h^{1/2}$ needs to be determined first; hence, the error bar curve of the transient current, corresponding to the $h^{1/2}$ of Specimens CIL01, CIL02, and CIL03, is drawn in Figure 4. The fitting results to the scatters show that the transient current increases negatively and exponentially with the height that the ball falls from. The relation can be expressed as:
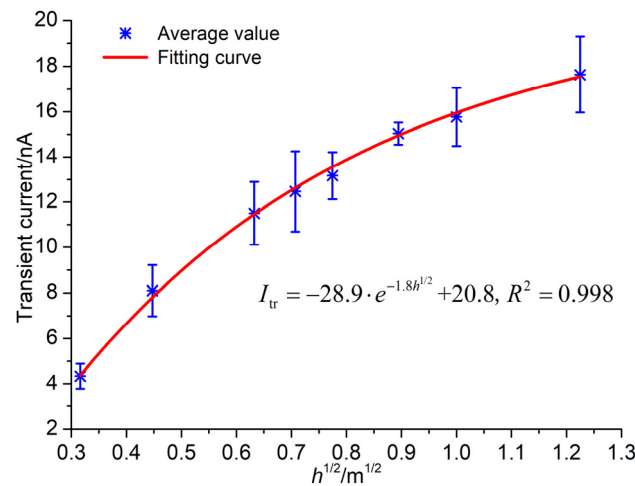
$$I_{tr} \propto -e^{-h^{1/2}} \tag{6}$$

Figure 4. Error bar curve of the transient currents with $h^{1/2}$ for the three groups of tests.

From Equations (5) and (6), we can derive Equation (7):

$$I_{tr} \propto -e^{-\mathrm{d}\varepsilon/\mathrm{d}t} \tag{7}$$

Equation (7) indicates that the weak current stimulated from coals under an impact load increases negatively and exponentially with the strain rate, which is consistent with that for coals under a static load [22,32].

The application of an impact load on the coal is completed in a very short time, which can be regarded as instantaneous, so the strain rate reaches its maximum instantly. The weak current increases with the strain rate, so the weak current reaches its peak value instantly, generating a transient current. After the application of the impact load, the coal deformation gradually recovers, so the weak current attenuates gradually and, finally, tends to be stable.

3.2. Attenuation Laws of Transient Currents

As depicted in Figure 2, the currents exhibit almost an identical attenuation trend. In order to facilitate the analysis of the unity of the attenuation law of the weak current, the time when the current begins to decay is zeroed. As shown in Figure 5, the weak current curves flatten out gradually, indicating that the decay rate of the current decreases. In addition, after hundreds of attenuations, these currents are still greater than the background one, indicating that the attenuation of currents is a slow dissipation process.
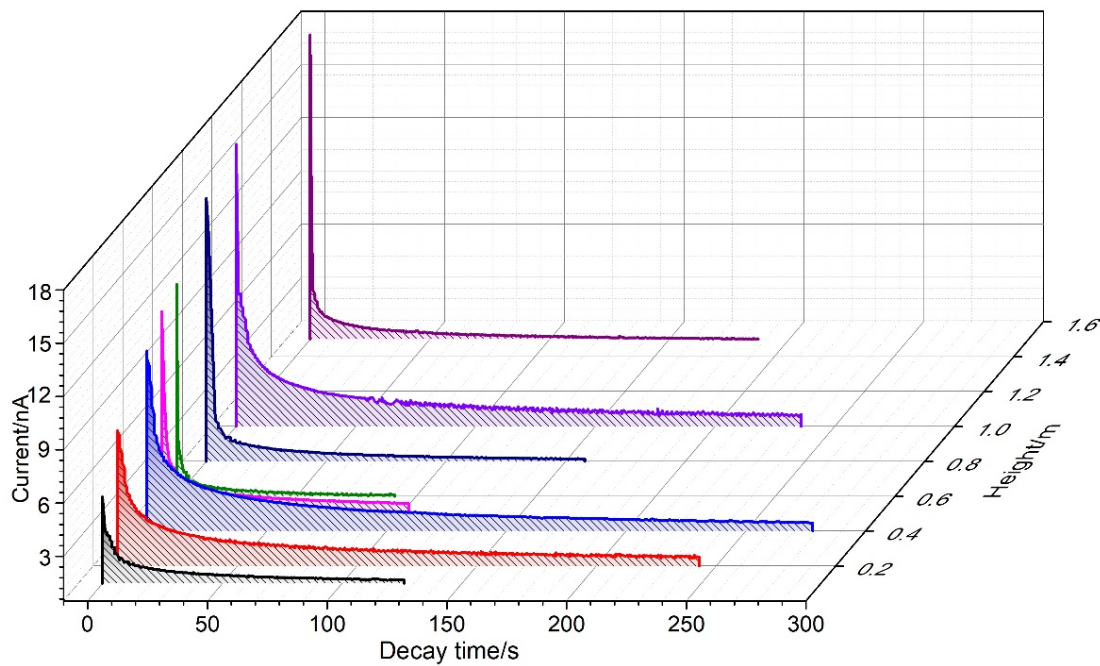
Figure 5. Curves of current attenuation for different ball falling heights for Specimen CIL02.

In 1988, Tsallis C proposed a non-extensive entropy (Tsallis entropy), which is defined as [33]:

$$S_q = k_B \frac{1 - \sum\limits_{i=1}^{W} P_i^q}{q - 1}$$ (8)

where k_B is Boltzmann's constant, P_i is a set of probabilities, q is the non-extensive parameter, and W is the total number of possible microscopic configurations. There is a normalization condition where $\sum\limits_{i=1}^{W} P_i = 1$. This kind of statistical mechanics, based on Tsallis entropy, is called non-extensive statistical mechanics, and it will be used to analyze the attenuation laws of the transient current.

Because both the transient currents and the stable currents are different for different ball falling heights, in order to unify the attenuation law of these currents, the decay currents are first normalized using the following formula:

$$\xi(t) = \frac{I_t - I_s}{I_p - I_s}$$ (9)

where $\xi(t)$ is the normalized current, I_t is the real-time current in the relaxation phase, and I_s is the stable current.

If the current relaxation was of the exponential type, then the normalized current $\xi(t)$ would satisfy the following equation [34–36]:

$$\frac{d\xi}{dt} = -\beta \cdot \xi$$ (10)

Considering the involvement of multi-fractality, a more general equation holds:

$$\frac{d\xi}{dt} = -\beta_q \cdot \xi^q$$ (11)

where β_q is the decay factor that is related to the internal energy of a system.

Equation (11) leads to a generalized *q*-exponential function:

$$\xi(t) = [1 - (1 - q)\cdot\beta_q\cdot t]^{1/1-q} = \exp(-\beta_q\cdot t) \tag{12}$$

The normalized currents after the withdrawal of the impact load on Specimen CIL02 are calculated by Equation (9). The scatters of ξ, corresponding to different heights, are depicted in Figure 6 and are fitted by using Equation (12). Figure 6 shows that all the fitting curves correspond well to the scatters of current measured in our experiments, and the coefficients of determination, R^2, are all greater than 0.95, showing that the fitting results are very good [37]. In addition, by non-extensive statistical mechanics, $q < 1$ enhances the rare events, while $q > 1$ enhances the frequent events. As shown in Figure 6, the q values are all greater than 2, indicating that the relaxation of these currents obeys the non-extensive statistical mechanics.
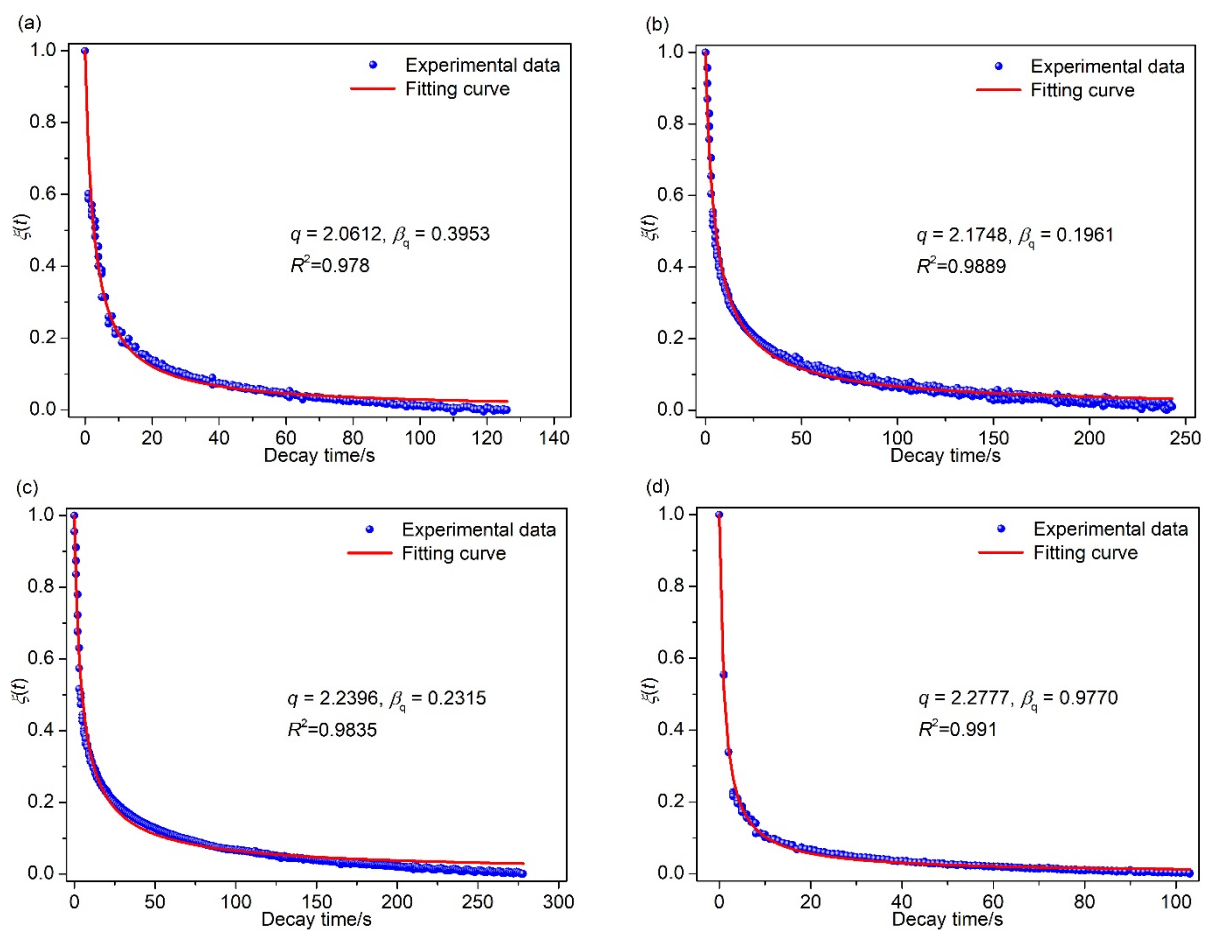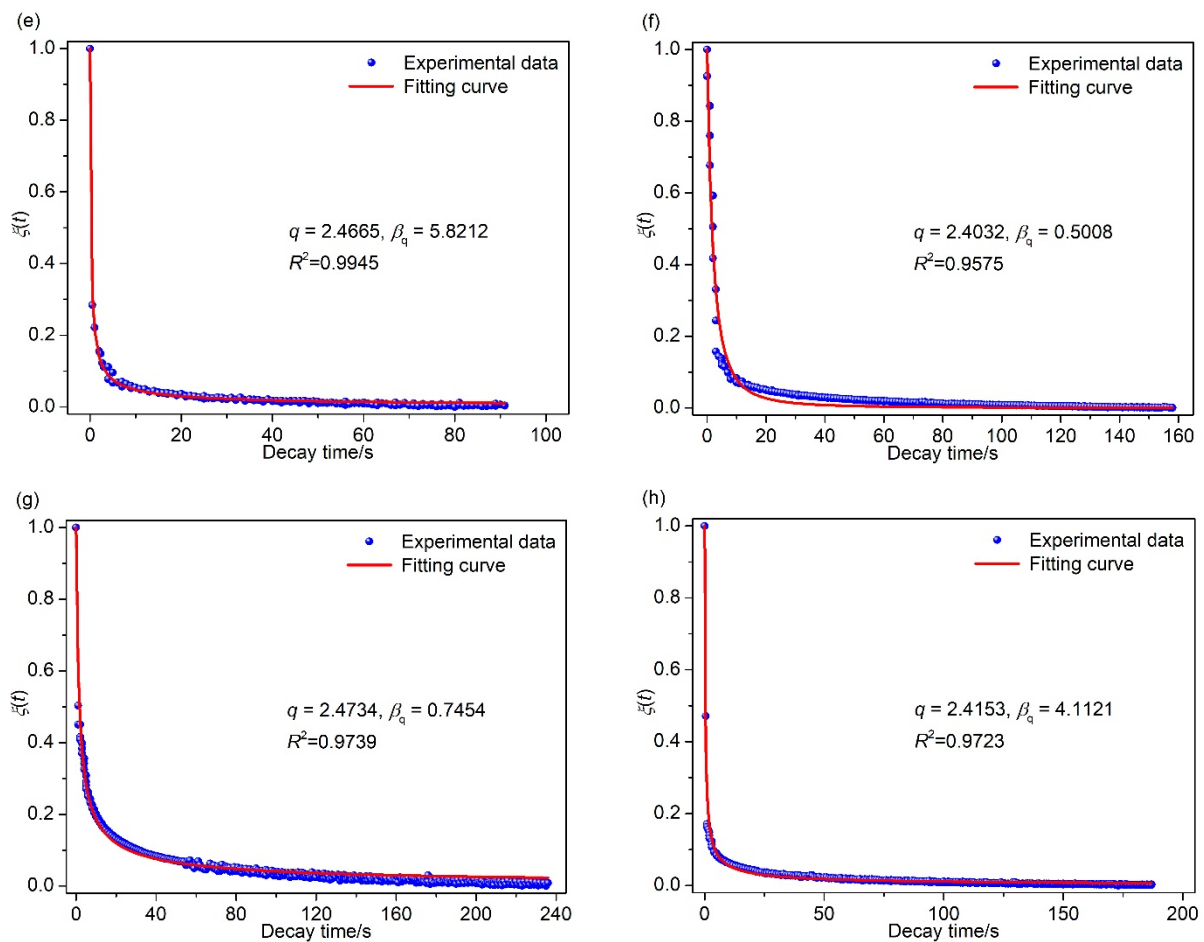

Figure 6. *Cont.*

Figure 6. Normalized decaying currents from Specimen CIL02 for different falling heights of the ball. (**a**) 0.1 m; (**b**) 0.2 m; (**c**) 0.4 m; (**d**) 0.5 m; (**e**) 0.6 m; (**f**) 0.8 m; (**g**) 1.0 m; (**h**) 1.5 m.

3.3. Mechanism of Weak Current from Loaded Coals

3.3.1. Carriers in Coal

The fact that the weak current can be stimulated from coals under an impact load shows that there must be carriers in the coal. According to the dielectric conduction theory, there are only three forms of carriers: ions, electrons, and holes [38].

Ionic conductivity is the conductive process of the directional movement of positive and negative ions, so the necessary condition for ionic conductivity is the presence of ions that can move freely [38]. The basis to judge whether there are ions that can move freely in a substance are: (1) whether there are ions and (2) whether there are conditions for ions to move freely. In our experiments, there is neither solution nor molten minerals in the dry coal sample at room temperature, so there is no condition for the free movement of ions. Therefore, it is inferred that the carriers of the weak current generated in the coal samples are not ions.

Freund et al. [18,19] proposed that the p-holes formed by the loss of an electron by the oxygen atom of silicate minerals are the main carriers in igneous rocks. Li et al. [22] introduced the p-hole theory to explain the generation mechanism of weak currents stimulated from coals under a static load and believed that the p-holes are induced by the breaking of covalent bonds within coal molecules. P-hole theory can well illustrate the directionality of weak currents, but there are still some limitations in using this theory. It holds that the p-holes in coals are not primary holes but are generated due to the fracture of chemical bonds. The existing research shows that a weak current can be generated the moment a load is applied to the coal/rock material, and it can still increase rapidly to a peak value even at a low stress level [14–16,18,22]. Considering that current is defined as the quantity

of charge passing through the cross-section of a conductor per unit of time [38], the sudden increase in current requires a large quantity of charge in a very short time. If the carriers of those currents are p-holes, then a large number of chemical bonds, such as –O–O–, –C–OH, –C–SH, –C–C_mH_n, in coals need to be broken quickly. However, the breaking of chemical bonds absorbs high energy, but the energy of the ball falling from a height of 0.1 m is too small to provide enough energy to break a large number of chemical bonds, so few p-holes can be activated and the transient current is impossible to stimulate. Therefore, p-holes are not the main carriers of the weak currents from stressed coals.

Based on the above analysis, the carriers of the weak current from loaded coal are electrons. Except for the free electrons that naturally exist in the coal, a large number of electrons can also be generated by friction, stress-induced polarization, and crack propagation, which will provide sufficient carriers for the weak currents from coals [32].

3.3.2. Mechanism and Physical Models

For the electrometer used in our experiments, the sign of the measured current is positive if it flows to the HI side. Our experimental results show that the weak currents measured are all positive, indicating that the current flows to the HI side of the electrometer. Accordingly, the diagram of the equivalent circuit, composed of the coal sample, copper electrodes, wires, and the electrometer, can be obtained, as shown in Figure 7. Considering that the flowing direction of electrons is opposite to that of the current [38], the electrons flow out from the HI side. Due to the movement of electrons being continuous in this circuit, the path that the electron moves along can be depicted in Figure 7, indicating that the electrons flow from the unstressed volume to the stressed one.
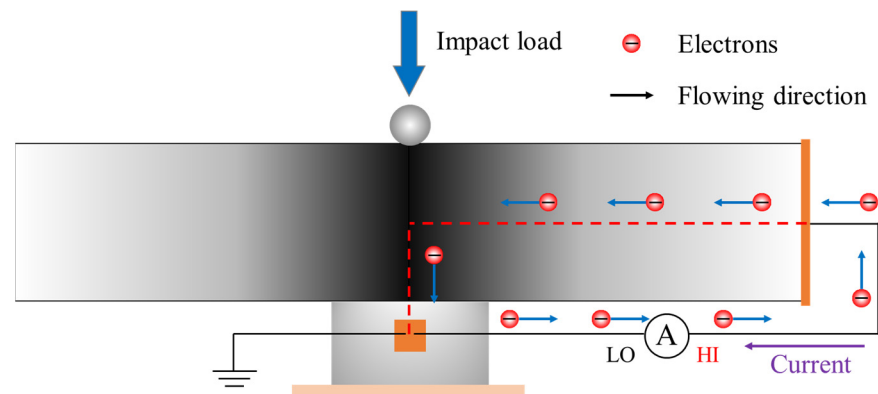

Figure 7. Equivalent circuit diagram showing the flow of the current and the movement of electrons in the coal.

Our previous research shows that the charge distribution in the coal and rock materials obeys the tip effect, which holds that electric charges tend to concentrate at the tip of a crack [30]. Therefore, the charge distribution on the coal surface is illustrated in Figure 8. The distribution of charges is closely related to the surface topography of the coal, and the surface of coal is rough, especially at the friction interface or surface of new cracks, so the charges cannot be evenly distributed. In fact, the negative charges are distributed on the surface of a "sunken" crack, while the positive charges are on that of a "bulge". In addition, under the action of the tip effect, the charges tend to concentrate at the tip location of the coal surface, so the electron density increases along the path to the tip of a "sunken" crack or a "bulge".
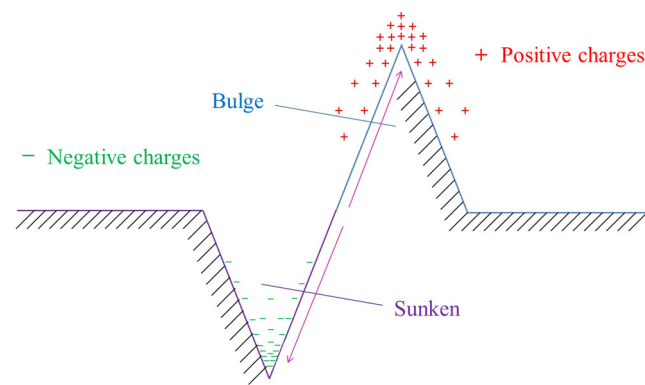
Figure 8. A physical model showing charge distribution on coal surfaces.

The coal is in the thermal equilibrium state when it is not loaded, so the free electrons are in a chaotic motion, representing electrical neutrality. As shown in Figure 9a, before the coal is loaded, the free electrons are evenly distributed in the coal, but when an impact load is applied to the coal (Figure 9b), the primary crack will be closed quickly, which is accompanied by the generation of a large quantity of charges due to friction electrification. Under the action of the tip effect of charges, the original and newly generated free electrons flow to the tip of the fracture space, leading to the reduction of free charge density in the loaded volume of the coal. Because of the charge density difference between the stressed volume and the unstressed one, the electrons in the unstressed volume will diffuse to the stressed volume through the conductive channel to reach a new charge balance in the coal. The diffusion path is depicted by the arrow in Figure 9b.
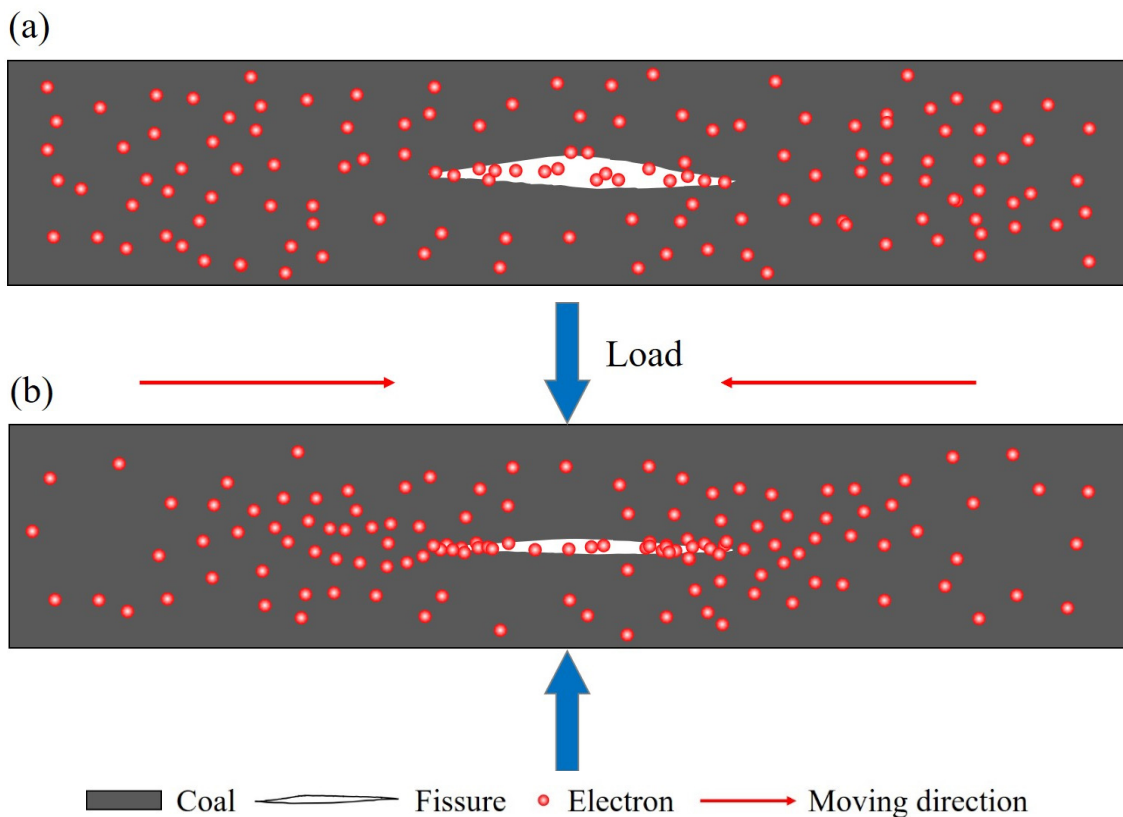

Figure 9. Schematic diagram showing the generation mechanism of currents induced by coal deformation. The coal is (**a**) unloaded and (**b**) loaded.

By definition, the current is calculated by [38]:

$$I = \frac{dq}{dt} \tag{13}$$

where I is the current, q is the charge quantity that flows from a cross-section of a conductor, and t is the time of charge flow.

The application of an impact load on coal can be regarded as instantaneous, making the primary cracks close in a very short time. Under these circumstances, the charge density difference is formed instantly, and the electrons flow instantaneously, so a transient current can be stimulated when an impact load is applied.

4. Conclusions

The contributions of this study can be summarized as follows:

(1) The moment an impact load is applied to coal, a weak current, increasing instantly to the peak value (transient current), is stimulated, and the current flows from the loaded volume to the unloaded one through the coal. The intensity of the transient current increases with impact velocity, which is positively related to the falling height of the ball.

(2) The transient current decays slowly after the withdrawal of the impact load, tending to be a stable value that is slightly greater than the background current before the load application. The attenuation of the transient current lasts hundreds of seconds and obeys non-extensive statistical mechanics, with the non-extensive parameter q greater than 2.

(3) The main carriers of the stimulated weak currents are free electrons. The generation mechanism of the weak currents induced by coal deformation is the instantaneous movement of electrons under a density difference. The closure of primary cracks makes electrons flow toward the tip of the shuttle fracture space under the action of the tip effect, leading to a charge density difference, which makes the electrons in the unloaded volume move to the loaded one to reach a new charge balance, generating the transient currents.

Author Contributions: D.L.: Conceptualization, Methodology, Investigation, Writing-Original Draft, Funding acquisition. E.W.: Writing-Review & Editing, Supervision, Funding acquisition. D.J.: Validation, Project administration. D.W.: Investigation, Formal analysis. W.L.: Software, Data curation. All authors have read and agreed to the published version of the manuscript.

Institutional Review Board Statement: Not applicable.

Informed Consent Statement: Not applicable.

Data Availability Statement: Data is available on request from the authors.

Conflicts of Interest: The authors declare no conflict of interest.

References

1. Keneti, A.; Sainsbury, B.A. Review of published rockburst events and their contributing factors. *Eng. Geol.* **2018**, *246*, 361–373. [CrossRef]
2. Cai, M. Principles of rock support in burst-prone ground. *Tunn. Undergr. Space Technol.* **2013**, *36*, 46–56. [CrossRef]
3. Feng, G.L.; Feng, X.T.; Xiao, Y.X.; Yao, Z.B.; Hu, L.; Niu, W.J.; Li, T. Characteristic microseismicity during the development process of intermittent rockburst in a deep railway tunnel. *Int. J. Rock Mech. Min. Sci.* **2019**, *124*, 104135. [CrossRef]
4. Jiang, Y.D.; Pan, Y.S.; Jiang, F.X.; Dou, L.M.; Ju, Y. State of the art review on mechanism and prevention of coal bumps in China. *J. China Coal Soc.* **2014**, *39*, 205–213.

5. Lawson, H.E.; Tesarik, D.; Larson, M.K.; Abraham, H. Effects of overburden characteristics on dynamic failure in underground coal mining. *Int. J. Rock Mech. Min. Sci.* **2017**, *27*, 121–129. [CrossRef]

6. Sepehri, M.; Apel, D.B.; Adeeb, S.; Leveille, P.; Hall, R.A. Evaluation of mining-induced energy and rockburst prediction at a diamond mine in Canada using a full 3D elastoplastic finite element model. *Eng. Geol.* **2020**, *266*, 105209. [CrossRef]

7. Yuan, L.; Jiang, Y.D.; He, X.Q.; Dou, L.M.; Zhao, Y.X.; Zhao, X.S.; Wang, K.; Yu, Q.; Lu, X.M.; Li, H.C. Research progress of precise risk accurate identification and monitoring early warning on typical dynamic disasters in coal mine. *J. China Coal Soc.* **2018**, *43*, 306–318.

8. Qiu, L.M.; Zhu, Y.; Song, D.Z.; He, X.Q.; Wang, W.X.; Liu, Y.; Xiao, Y.Z.; Wei, M.H.; Yin, S.; Liu, Q. Study on the nonlinear characteristics of EMR and AE during coal splitting tests. *Minerals* **2022**, *12*, 108. [CrossRef]

9. Qiu, L.M.; Liu, Z.T.; Wang, E.Y.; He, X.Q.; Feng, J.J.; Li, B.L. Early-warning of rock burst in coal mine by low-frequency electromagnetic radiation. *Eng. Geol.* **2020**, *279*, 105755. [CrossRef]

10. Vallianatos, F.; Tzanis, A. Electric current generation associated with the deformation rate of a solid: Preseismic and coseismic signals. *Phys. Chem. Earth* **1998**, *23*, 933–939. [CrossRef]

11. Stavrakas, I.; Anastasiadis, C.; Triantis, D.; Vallianatos, F. Piezo stimulated currents in marble samples: Precursory and concurrent-with-failure signals. *Nat. Hazards Earth Syst. Sci.* **2003**, *3*, 243–247. [CrossRef]

12. Stavrakas, I.; Kourkoulis, S.; Triantis, D. Damage evolution in marble under uniaxial compression monitored by pressure stimulated currents and acoustic emissions. *Fract. Struct. Integr.* **2019**, *13*, 573–583. [CrossRef]

13. Triantis, D.; Stavrakas, I.; Anastasiadis, C.; Kyriazopoulos, A.; Vallianatos, F. An analysis of pressure stimulated currents (PSC), in marble samples under mechanical stress. *Phys. Chem. Earth* **2006**, *31*, 234–239. [CrossRef]

14. Freund, F.T.; Takeuchi, A.; Lau, B.W. Electric currents streaming out of stressed igneous rocks—A step towards understanding pre-earthquake low frequency EM emissions. *Phys. Chem. Earth* **2006**, *31*, 389–396. [CrossRef]

15. Freund, F.; Ouillon, G.; Scoville, J.; Sornette, D. Earthquake precursors in the light of peroxy defects theory: Critical review of systematic observations. *Eur. Phys. J.-Spec. Top.* **2021**, *230*, 7–46. [CrossRef]

16. Li, D.X.; Wang, E.Y.; Li, Z.H.; Ju, Y.Q.; Wang, D.M.; Wang, X.Y. Experimental investigations of pressure stimulated currents from stressed sandstone used as precursors to rock fracture. *Int. J. Rock Mech. Min. Sci.* **2021**, *145*, 104841. [CrossRef]

17. Kyriazopoulos, A.; Anastasiadis, C.; Triantis, D.; Brown, C.J. Non-destructive evaluation of cement-based materials from pressure-stimulated electrical emission—Preliminary results. *Constr. Build. Mater.* **2011**, *25*, 1980–1990. [CrossRef]

18. Freund, F.T. Pre-earthquake signals: Underlying physical processes. *J. Asian Earth Sci.* **2011**, *41*, 383–400. [CrossRef]

19. Scoville, J.; Sornette, J.; Freund, F.T. Paradox of peroxy defects and positive holes in rocks Part II: Outflow of electric currents from stressed rocks. *J. Asian Earth Sci.* **2015**, *114*, 338–351. [CrossRef]

20. He, M.; Li, Z.H.; Liu, J.; Liu, Y.J. Experimental study on surface current of coal under uniaxial compression. *J. China Coal Soc.* **2013**, *38*, 966–969.

21. Li, Z.H.; Wang, E.Y.; He, M. Laboratory studies of electric current generated during fracture of coal and rock in rock burst coal mine. *J. Min.* **2015**, *2015*, 235636. [CrossRef]

22. Li, D.X.; Wang, E.Y.; Ju, Y.Q.; Wang, D.M. Laboratory investigations of a new method using pressure stimulated currents to monitor concentrated stress variations in coal. *Nat. Resour. Res.* **2021**, *30*, 707–724. [CrossRef]

23. Li, D.X.; Wang, E.Y.; Yue, J.H.; Zhang, X.; Wang, D.M.; Ju, Y.Q. A weak current technique for coal and rock dynamic disaster prediction and its application. *Chin. J. Rock Mech. Eng.* **2022**, *4*, 764–774.

24. Kong, X.G.; He, D.; Liu, X.F.; Wang, E.Y.; Li, S.G.; Liu, T.; Ji, P.F.; Deng, D.Y.; Yang, S.R. Strain characteristics and energy dissipation laws of gas-bearing coal during impact fracture process. *Energy* **2022**, *242*, 123028. [CrossRef]

25. Kong, X.G.; Wang, E.Y.; Li, S.G.; Lin, H.F.; Xiao, P.; Zhang, K.Z. Fractals and chaos characteristics of acoustic emission energy about gas-bearing coal during loaded failure. *Fractals* **2019**, *27*, 1950072. [CrossRef]

26. Liu, G.J.; Mu, Z.L.; Du, J.L. Investigation of coal burst characteristics under impact loading. *Int. J. Oil Gas Coal Technol.* **2018**, *18*, 118–145. [CrossRef]

27. Feng, X.J.; Ding, Z.; Ju, Y.Q.; Zhang, Q.M.; Ali, M. "Double peak" of dynamic strengths and acoustic emission responses of coal masses under dynamic loading. *Nat. Resour. Res.* **2022**, *31*, 1705–1720. [CrossRef]

28. Yang, S.L.; Yue, H.; Chen, X.L.; Zhai, R.H.; Zhang, S. Experimental study on damage evolution characteristics of coal samples under impact load under different surrounding pressures. *Lithosphere* **2022**, *S11*, 106154. [CrossRef]

29. Xu, X.M.; Wang, Q.; Liu, H.; Zhao, W.W.; Zhang, Y.H.; Wang, C. Experimental investigation on the characteristics of transient electromagnetic radiation during the dynamic fracturing progress of gas-bearing coal. *J. Geophys. Eng.* **2020**, *17*, 799–812. [CrossRef]

30. Barton, N. Suggested methods for the quantitative description of discontinuities in rock masses. International Society for Rock Mechanics. *Int. J. Rock Mech. Min. Sci. Geomech. Abstr.* **1978**, *15*, 319–368.

31. Feynman, R. *The Feynman Lectures on Physics*; Addison Wesley: Boston, MA, USA, 1970; Volume I.

32. Li, D.X. *Study on the Weak Current Effect and Its Mechanism of Stressed Coal during Damage*; China University of Mining and Technology: Xuzhou, China, 2021.

33. Tsallis, C. Possible generalization of Boltzmann-Gibbs statistics. *J. Stat. Phys.* **1988**, *52*, 479. [CrossRef]

34. Vallianatos, F.; Triantis, D. Is pressure stimulated current relaxation in amphibolite a case of non-extensivity? *Europhys. Lett.* **2012**, *99*, 18006. [CrossRef]

35. Vallianatos, F.; Triantis, D. A non-extensive view of the Pressure Stimulated Current relaxation during repeated abrupt uniaxial load-unload in rock samples. *Europhys. Lett.* **2013**, *104*, 68002. [CrossRef]
36. Stergiopoulos, C.; Stavrakas, I.; Triantis, D.; Vallianatos, F.; Stonham, J. Predicting fracture of mortar beams under three-point bending using non-extensive statistical modeling of electric emissions. *Physica A* **2015**, *419*, 603–611. [CrossRef]
37. Li, D.X.; Wang, E.Y.; Kong, X.G.; Ali, M.; Wang, D.M. Mechanical behaviors and acoustic emission fractal characteristics of coal specimens with a pre-existing flaw of various inclinations under uniaxial compression. *Int. J. Rock Mech. Min. Sci.* **2019**, *116*, 38–51. [CrossRef]
38. Fischer-Cripps, A.C. *The Electronics Companion*; CRC Press: Boca Raton, FL, USA, 2004.